Translational Oncology
www.transonc.com

Volume 3 Number 6 December 2010 pp. 380–388 380

Nitric Oxide–Mediated Tumoricidal Activity of Murine Microglial Cells[1,2]

Emily C. Brantley[3], Lixia Guo[3], Chenyu Zhang[4], Qingtang Lin, Kenji Yokoi, Robert R. Langley, Ewa Kruzel, Marva Maya, Seung Wook Kim, Sun-Jin Kim, Dominic Fan and Isaiah J. Fidler

Department of Cancer Biology, Cancer Metastasis Research Center, The University of Texas MD Anderson Cancer Center, Houston, TX, USA

Abstract

Experimental metastases in the brain of mice are infiltrated by microglia, and parabiosis experiments of green fluorescent protein (GFP^+) and GFP^- mice revealed that these microglia are derived from circulating monocytes (GFP^+, $F4/80^+$, and $CD68^+$). These findings raised the question as to whether microglia (specialized macrophages) possess tumoricidal activity. C8-B4 murine microglia cells were incubated *in vitro* in medium (control) or in medium containing both lipopolysaccharide and interferon-γ. Control microglia were not tumoricidal against a number of murine and human tumor cells, whereas lipopolysaccharide/interferon-γ–activated microglia lysed murine and human tumor cells by release of nitric oxide. Parallel experiments with murine peritoneal macrophages produced identical results. Neither activated microglia nor activated macrophages lysed nontumorigenic murine or human cells. Collectively, these data demonstrate that brain metastasis–associated microglia are derived from circulating mononuclear cells and exhibit selective and specific tumoricidal activity.

Translational Oncology (2010) 3, 380–388

Introduction

Throughout the body, the connective tissue not only plays a tissue-supportive role but also embeds host-defense cells that are capable of phagocytosing foreign materials, microorganisms, and dead cells. In the absence of connective tissue in the brain, the surveillance functions must be performed by cells that are similar to macrophages in other organs [1]. In humans, under normal conditions, microglia are small cells evenly distributed within the white and gray matter that make up approximately 5% of the glial populations in the white matter of the corpus callosum [1,2]. In mice, more microglia are localized in the gray matter than in the white, particularly in the hippocampus, olfactory telencephalon, basal ganglia, and substantia nigra. The proportion of the resident microglia populations in the adult mouse brain varies from 5% in the cortex and corpus callosum to 12% in the substantia nigra [2]. These so-called "resting" microglia were once thought to be largely inactive; however, recent work describes their active patrol of the healthy brain, using their motile processes to constantly survey the microenvironment [3,4]. It is under pathologic conditions, such as injury or inflammation, that immediate and drastic changes take place among microglia, that is, their nucleus and cytoplasm enlarge, they acquire the ability to divide, and they rapidly become mobile and phagocytose materials [2–4].

Microglia are generally considered to be brain macrophages that are derived from monocytes and colonized by way of circulating monocyte invasion into the brain on pathologic developments such as apoptosis of neurons [1,5]. Microglia and macrophages share molecular markers such as MAC1, F4/80, and FcIgG1/2b [6,7]. It is largely recognized that some microglia develop from a pool of blood monocytes and can colonize the brain early in development [8–10]. Lipopolysaccharide (LPS) and interferon-γ (IFN-γ)–activated microglia isolated from the adult brain are more similar to macrophages infiltrating the central nervous system (CNS) than naive microglia of the brain [11]. Moreover,

Address all correspondence to: Isaiah J. Fidler, DVM, PhD, Department of Cancer Biology, Cancer Metastasis Research Center, The University of Texas MD Anderson Cancer Center, Unit 854, 1515 Holcombe Blvd, Houston, TX 77030. E-mail: ifidler@mdanderson.org

[1]This work was supported in part by Cancer Center Support Core grants CA16672 and 1U54CA143837 from the National Cancer Institute, National Institutes of Health.
[2]There is no conflict of interest with any author or product used in this translational research study.

[3]These authors contributed equally to this work.
[4]Current address: Department of Molecular and Cellular Oncology, The University of Texas MD Anderson Cancer Center, Houston, TX.

Received 26 July 2010; Revised 16 August 2010; Accepted 18 August 2010

 1944-7124/10/$25.00
DOI 10.1593/tlo.10208

LPS has been shown to extend the life span of cultured mouse microglia by increasing the expression of Bcl-xl and suppressing the induction of apoptosis and autophagy [12].

The role of macrophages and microglia in tumorigenesis is widely disputed. A large body of evidence suggests that in some situations, macrophages can promote tumor growth, metastasis, and angiogenesis [13,14], whereas in others, macrophages are tumoricidal by selectively recognizing and destroying tumor cells [15–18]. Data suggest that these behavioral changes are largely dependent on the context of the specific tumor type and its microenvironment [19–22]. Although the presence of macrophages and microglia has been reported in both clinical and experimental specimens of brain metastasis, their exact function is unclear [23–30]. To determine whether, similar to macrophages [13–15], microglia can be activated to the tumoricidal state, we incubated normal (control) and activated C8-B4 murine microglia [6] or murine macrophages with several nontumorigenic and tumorigenic murine and human cells. We report that activated microglia behave similarly to macrophages by inducing cytotoxicity in a variety of tumor cells, but not in nontumorigenic cells, through the release of nitric oxide (NO).

Materials and Methods

Cell Line and Culture Conditions

The spontaneously immortalized murine C8-B4 microglial cell line [6] was the gift of Dr D. Trisler (The University of Maryland, College Park, MD). The PC14P human lung adenocarcinoma cell line [31] was obtained from Dr N. Saijo (National Cancer Center Research Institute, Tokyo, Japan). The B16-BL6 cell line is a highly metastatic and invasive variant [32,33] derived from B16 mouse melanoma [34]. The K-1735 C4 melanoma syngeneic to C3H-/HeN mice [35] was a gift from Dr M. L. Kripke (MD Anderson Cancer Center, Houston, TX). The MDA-MB-231 is an ER-negative human breast carcinoma cell line [36] and was a gift from Dr R. Cailleau (Department of Medicine, MD Anderson Cancer Center). The immortalized murine brain endothelial cell line was a gift from Dr R. R. Langley (MD Anderson Cancer Center) [37]. It was isolated from a transgenic mouse whose tissues harbor a temperature-sensitive SV40 large T antigen (*H-2K^b-ts*A58 mouse) [5,26]. The immortalized murine astrocyte cell line was established by our laboratory also from the *H-2K^b-ts*A58 mouse [26]. The immortalized murine astrocyte and brain endothelial cell lines were maintained in high-glucose Dulbecco minimal essential medium supplemented with 10% fetal bovine serum (FBS), 2 mM L-glutamine, sodium pyruvate, nonessential amino acids, and vitamin solution (Life Technologies, Inc, Rockville, MD), at the permissive temperature of 33°C in 8% CO_2. The 3LL-LM cell line is the Lewis lung carcinoma syngeneic to the C57BL/6 mice [11]. Unless otherwise stated, all tumor cell lines were maintained as adherent monolayer cultures in Eagle minimum essential medium supplemented with 10% FBS (Thermo Fisher Scientific HyClone, Logan, UT), L-glutamine, pyruvate, nonessential amino acids, two-fold vitamins, and penicillin-streptomycin (GIBCO/Invitrogen, Carlsbad, CA) and incubated at 37°C in 6.4% CO_2 with balance of air. The C8-B4 line was maintained in Dulbecco minimal essential medium supplemented with 10% FBS, 2 mM L-glutamine, sodium pyruvate, nonessential amino acids, and vitamin solution (Life Technologies, Inc). All reagents used for tissue culture were free of endotoxin as determined by the Limulus amebocyte lysate assay (Associates of Cape Cod, Woods Hole, MA), and all cell lines were free of *Mycoplasma* spp, Sendai virus, mouse hepatitis virus, pneumonia virus of mice, minute virus of mice, mouse parvovirus (MPV1, MPV2, and MPV3), Theiler's murine encephalomyelitis virus, murine norovirus, reovirus type 3, mouse rotavirus, ectromelia virus, lymphocyte choriomeningitis virus, polyoma virus, lactate dehydrogenase–elevating virus, mouse adenovirus (MAD1 and MAD2), mouse cytomegalovirus, K virus, mouse thymic virus, and Hantaan virus (assayed by the Research Animal Diagnostic Laboratory, University of Missouri, Columbia, MO). Cells used in this study were from frozen stock, and all experiments were performed within 10 *in vitro* passages after thawing.

Animals

Female transgenic green fluorescent mice (C57BL/6-Tg [ACTB-EGFP]10sb/J) were purchased from Jackson Laboratory (Bar Harbor, ME). The mice were housed and maintained under specific pathogen-free conditions. Age-matched female C57BL/6 mice were purchased from the Animal Production Area of the National Cancer Institute, Frederick Cancer Research Facility (Frederick, MD). Animal facilities were approved by the American Association for Accreditation of Laboratory Animal Care and met all current regulations and standards of the US Department of Agriculture, US Department of Health and Human Services, and the National Institutes of Health. The mice were used in accordance with institutional guidelines when they were 8 to 10 weeks old.

Parabiosis

To identify cells infiltrating metastases in the brain parenchyma and investigate their origin, we used a parabiosis model system. A transgenic female green fluorescent mouse and a female C57BL/6 (wild-type) mouse were anesthetized with pentobarbital (0.5 mg/g body weight; Abbott Laboratories, Chicago, IL). Opposing sides of the bodies were shaved. The skin was cleaned with iodine and alcohol and was widely excised from the shoulder (humerus) joint to the hip (femur) joint. The muscle layer was separated by dissection. The two mice were then anastomosed as follows: the muscle layer of each mouse was approximated by interrupted absorbable sutures (4-0 vicryl; Ethicon, Inc, Somerville, NJ) and then was sutured skin to skin by continuous nonabsorbable suture (4-0 prolene; Ethicon, Inc). Additional continuous anchoring suture to secure the anastomosis was placed over the anastomosis site. The parabionts were wrapped with elastic band to relieve wound tension. Establishment of common circulation was confirmed as previously described 2 weeks after the procedure [38].

To minimize postoperative pain, analgesia was used for all mice as per the University of Texas MD Anderson Cancer Center Institutional Animal Care and Use Committee Standard Operating Procedures based on the US Department of Agriculture Animal Welfare Act Regulations and PHS Policy. The nonsteroidal anti-inflammatory agent carprofen (Rimadyl; Pfizer Animal Health, New York, NY) was given to all our animals postoperatively as 5 mg/7.5-ml gelatin cubes for 2 to 3 days.

Injection of Mouse Lung Cancer Cells (3LL) into the Internal Carotid Artery

To produce metastatic tumors in the brain, 3LL cells were harvested from subconfluent cultures by a 2-minute exposure to 0.25% trypsin and 0.02% EDTA. Then, medium containing 10% FBS was added, and the cells were washed once in serum-free medium and resuspended with the adjustment of the number of cells to 2.5×10^4 in 100 μl of Ca^{2+}- and Mg^{2+}-free Hank's balanced salt solution (HBSS). Cell viability was determined by trypan blue exclusion, and only single-cell suspensions of greater than 95% viability were used for injection. Both mice of parabionts were anesthetized by intraperitoneal injection of

pentobarbital sodium (0.5g/kg of body weight; Nembutal; Abbott Laboratories), restrained on a corkboard on the back, and placed under a dissecting microscope. The head of the wild-type mouse was stabilized (on the corkboard) with a rubber band placed between the teeth of the upper jaw. The hair over the trachea was shaved, the neck was prepared for surgery with alcohol-iodine, and the skin was cut by a mediolateral incision. After blunt dissection, the trachea was exposed. The muscles were separated to expose the right common carotid artery, which was then separated from the vagal nerve. The artery was prepared for an injection distal to the point of division into the internal and external carotid arteries. A ligature of 5-0 silk suture was placed in the distal part of the common carotid artery. A second ligature was placed and tied proximal to the injection site. The artery was nicked with a pair of microscissors, and a less-than-30-gauge glass cannula was inserted into the lumen. To ensure proper delivery, the cells were injected slowly, and the cannula was removed. The second ligature was tightened, and the skin was closed by sutures. To inject cells into the internal or external carotid artery, the glass cannula was threaded into the internal or external carotid artery, respectively. All intracarotid artery injections were always done under a dissecting microscope, and all required a glass cannula with a diameter smaller than 30 gauge. We prepared such cannulas from 1-mm-diameter glass capillary tubes that were heated and then stretched. The diameter could be varied by varying the amount of stretching, and each cannula could be used repeatedly. The cannula was fixed to a 1-ml plastic syringe by melting the hub around the cannula [39].

Necropsy and Tissue Processing

Three weeks after the intracarotid injection, the wild-type (tumor-bearing) mice were separated from the transgenic green fluorescent mice (C57BL/6-Tg [ACTB-EGFP] 10sb/J) that were killed. The wild-type mice were allowed to survive, but when they became moribund, they were killed by injecting an excessive dose of Nembutal (1 g/kg of body weight). The skull was opened, and the brain was harvested and embedded in an optimal cutting temperature compound (Miles, Elkhart, IN) for frozen sectioning.

Immunohistochemistry

C8-B4 microglia were plated at a density of 2×10^5 cells/chamber in four-chambered slides. The following day, cells were fixed in 4% paraformaldehyde and washed with PBS. The samples were blocked briefly in 5% normal horse serum + 1% normal goat serum in PBS and then incubated at 4°C with an antibody directed against either CD68, Iba-1, or F4/80 (1:200 each) overnight. The slides were subsequently washed three times with PBS and then incubated with appropriate peroxidase-conjugated secondary antibody for 1 hour at room temperature. The slides were then rinsed with PBS and incubated with diaminobenzidine (Research Genetics, Huntsville, AL). The cells were visualized using an Olympus microscope (BX-51) with a DPTI digital camera (Olympus, Center Valley, PA).

Colocalization of F4/80 and CD68

Frozen tissues in the optimal cutting temperature compound were sectioned (6-8 μm), mounted on positively charged slides, and air-dried for 30 minutes. The sections were fixed in cold acetone for 10 minutes and then washed three times with PBS for 3 minutes each. Double staining for F4/80 and CD68 required a protein block with 5% normal horse serum and 1% normal goat serum for 5 minutes. Rabbit anti-human CD68 polyclonal antibody (sc-9139; Santa Cruz Biotechnology, Inc, Santa Cruz, CA) was applied at a 1:100 dilution in blocking solution. After overnight incubation at 4°C, the slides were washed three times with PBS for 3 minutes each time. Sections were blocked for 5 minutes at room temperature, and goat antirabbit A594 antibody (A11037; Invitrogen Corp) was added at a 1:600 dilution and incubated in blocking solution for 1 hour at room temperature. The slides were then washed three times for 3 minutes each time with PBS. Sections were blocked again for 5 minutes and incubated at 4°C with rat anti-mouse F4/80 monoclonal antibody (1:100 dilution; Serotec, Raleigh, NC) in blocking solution overnight at 4°C. Tissue sections were then washed three times with PBS for 3 minutes. Protein blocking was performed for 5 minutes, and goat antirat Cy-3 antibody (GxRt-Cy3; Jackson Immunoresearch, West Grove, PA) was added at a 1:600 dilution and incubated for 1 hour in blocking solution at room temperature. The slides were washed three times for 3 minutes each time with PBS, and nuclei were stained at room temperature for 10 minutes with Hoechst 33342 (Molecular Probes, Carlsbad, CA). The slides were then washed three times with PBS for 3 minutes each time. Cover slips were placed on top of the slides using glycerol in PBS with fluorescent mounting medium (propyl gallate; Acros Organics, Morris Plains, NJ). Images were captured with an Olympus microscope (BX-51) with an attached DP71 digital camera and processed with DP Controller and DPManager software (Olympus, Center Valley, PA). Color codes detecting cells were green for cells from transgenic green fluorescent mice (C57BL/6-Tg [ACTB-EGFP]10sb/J), red for cells expressing CD68, blue for expressing F4/80, and gray for nuclei [38].

Peritoneal Exudate Macrophage Isolation

Peritoneal exudate macrophages (PEMs) were collected by peritoneal lavage, in 10 ml of 37°C calcium-free and magnesium-free HBSS, from C57BL/6 mice given intraperitoneal injections of 1.5 to 2.0 ml of sterile thioglycollate broth (Baltimore Biological Laboratories, Cockeysville, MD) 4 to 5 days before harvest. The lavage returns were centrifuged at 200*g* for 10 minutes at room temperature, and the cells were resuspended in serum-free medium, seeded at 100,000 cells/well into 96-well tissue culture plates (Falcon 3072 Microtest III; Becton Dickinson, Lincoln Park, NJ), and allowed to attach to plastic at 37°C for 45 minutes. Nonadherent cells were removed by rinsing the wells with HBSS, and the cells were refed with fresh complete minimal essential medium. The monolayers routinely contained greater than 98% pure peritoneal macrophages as assessed by morphologic and phagocytic criteria [40].

Tritiated Thymidine Assay

Log-phase target tumor cells were plated at a density of 3×10^5 and incubated overnight to allow attachment. The following day, 1×10^5 C8-B4 microglia or C57BL/6 peritoneal macrophages were plated per well in a 96-well plate and tumor cells were labeled with 3 μCi of ^{3}H-thymidine for 18 hours. On day 3, macrophages were activated with a combination of IFN-γ (10 ng/ml) and LPS (100 ng/ml) for at least 2 hours. Microglia were either left untreated or were treated with one of the following: vascular endothelial growth factor (50 ng/ml), interleukin-6 (IL-6; 50 ng/ml), IL-8 (50 ng/ml), or a combination of IFN-γ (10 ng/ml) and LPS (100 ng/ml) for at least 2 hours. For the inducible NO synthase (iNOS) inhibitor, N^G-monomethyl-L-arginine (NMA; Sigma, St Louis, MO), microglia were pretreated for 2 hours with 3 mM NMA before IFN-γ and LPS activation. After treatment, 2×10^4 ^{3}H-labeled tumor cells were added to both of the untreated microglia and/or macrophages as well as the cytokine-treated microglia

and/or macrophages. As a control, ^{3}H-labeled tumor cells were also cultured alone. All cultures were done in triplicate. Microglia and/or macrophages and tumor cells were incubated for an additional 72 hours when the cells were lysed with 100 µl of 0.1 M KOH, and radioactivity was measured using a scintillation counter. Percentage cytotoxicity was calculated as a ratio to ^{3}H-labeled tumor cells cultured alone.

Assay for Nitrite Production

Nitrite accumulation in the culture supernatant was measured in a colorimetric assay as described previously [41]. At different times, 50-µl aliquots of supernatants were mixed with equal volumes of Griess reagent (1% sulfanilamide and 0.1% napthylenediamine dihydrochloride in 2.5% phosphoric acid). The mixtures were incubated for 10 minutes with shaking, and A565 was measured with the use of a microplate reader. The concentration of nitrite was determined by comparing it with a standard solution of sodium nitrite in medium [41].

Statistical Analysis

Levels of significance for comparison between samples were determined by Student's *t* test distribution. $P \leq .05$ was considered to be statistically significant.

Results

In the first set of experiments, we examined metastases in the brain of nude mice injected in the carotid artery with murine 3LL cells 4 weeks before the histology-immunohistochemistry evaluations. As can be seen in Figure 1, the metastases were infiltrated by a large number of cells expressing microglia markers F4/80, CD68, and ionizing calcium-binding adapter molecule-1 (Iba-1).

Because microglia and PEM exhibit nearly identical markers, we wished to determine whether microglia originate from circulating monocytes that also give rise to PEM. To do so, we examined the presence of microglia in a brain metastasis model established in a C57BL/6 (wild-type) mouse parabiosed to a transgenic green fluorescent mouse (C57BL/6-GFP^{+}). This parabiosis model allows for the visualization of infiltrating cells to the brain (Figure 2). Reconstituting mice with a single injection of GFP^{+} bone marrow cells will largely home to the liver and lungs; therefore, we used the parabiosis model, which allows for continuous release of bone marrow cells into the circulation [42]. Mouse 3LL lung tumor cells formed metastases in the brains of wild-type mice, and these lesions were infiltrated by cells originating from both the C57BL/ 6-GFP^{+} mouse and the wild-type mouse. Infiltrating cells were identified as follows: 1) cells from wild-type expressing either CD68 or Iba-1 (red), 2) cells from wild-type expressing F4/80 (blue), 3) cells from wild-type expressing CD68/Iba-1 and F4/80 (pink), 4) cells from C57BL/6-GFP^{+} expressing neither F4/80 nor CD68/Iba-1 (green), 5) cells from C57BL/6-GFP^{+} expressing CD68/Iba-1 (yellow), 6) cells from C57BL/6-GFP^{+} expressing F4/80 (sky blue), and 7) cells from C57BL/6-GFP^{+} expressing CD68/Iba-1 and F4/80 (white). Data shown in Figure 2 suggest that circulating monocytes expressing CD68/Iba-1 and/or F4/80 infiltrate into the brain metastases. Importantly, a number of non-GFP^{+} cells were also found to express CD68/Iba-1 and F4/80 either alone or in combination, suggesting that the population of resident microglia are also either recruited or expanded in response to the metastatic brain lesion.

Next, we confirmed the identity of the immortalized C8-B4 murine microglia cells by examining these cells for classic microglial/macrophage markers, including Iba-1, F4/80, and CD68. Immunohistochemical analysis of these cells revealed strong expression of these antigens in both microglia and macrophages. In addition, to assess the functional ability of the microglial cells to phagocytose, they were cultured with polystyrene-coated beads and analyzed for their ability to ingest the blue-labeled beads. The phagocytic activity of C8-B4 microglia has been shown previously [6], and we confirmed this characteristic behavior as well (data not shown).

Both macrophages and microglia can be potently activated by IFN-γ and LPS to express a variety of integral cell surface proteins necessary for immune function [16,43]. Importantly, LPS + IFN-γ–activated microglia isolated from the adult brain are similar to CNS-infiltrating macrophages [11], and recent data suggest that LPS confers a survival advantage to cultured mouse microglia by simultaneously increasing the expression of Bcl-xl and suppressing the induction of apoptosis and autophagy of the microglia [12]. We compared the tumoricidal activity of microglia pretreated with numerous cytokines against melanoma cells. Treatment of microglia with a combination of LPS and IFN-γ induced a significant increase in cytotoxicity against both B16-BL6 and K-1735 melanoma tumor cells (data not shown). In contrast, pretreatment of microglia with vascular endothelial growth factor, IL-6, or IL-8 had no significant effect on microglial-mediated cytotoxicity against melanoma cells (data not shown). In addition, to rule out cytotoxicity induced by nutrient deprivation, we performed the same experiment using various cell types of normal origin, instead of microglia. LPS + IFN-γ–treated fibroblasts, astrocytes, and brain endothelial cells failed to induce cytotoxicity in the B16-BL6 tumor cells (data not shown). The induction of cytotoxicity was, therefore, unique to LPS + IFN-γ–activated microglia.

The ability of activated macrophages to induce cytotoxicity of tumor cells has been recognized for more than 30 years [16]. Using the B16-BL6

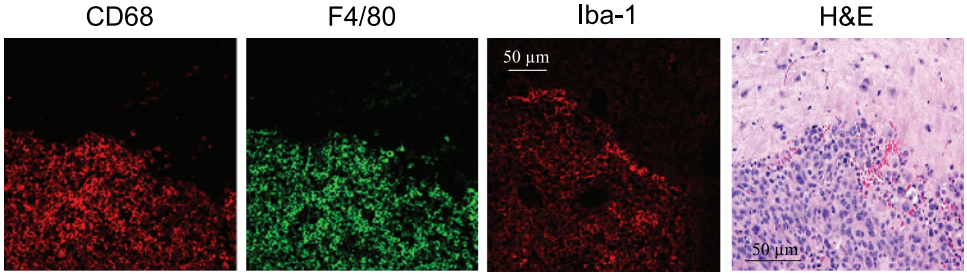

Figure 1. Microglia infiltrating into experimental brain metastases. 3LL lung cancer cells were injected in the carotid artery of nude mice. Four weeks later, the mice were killed, and the brain tissue was harvested, processed, and stained with hematoxylin and eosin to verify tumor location. Specific antibodies were then applied to frozen, fixed brain tissue sections, and immunohistochemical analysis of the resulting tumors revealed F4/80^{+}, CD68^{+}, and Iba-1^{+} cells infiltrating the experimental metastases.

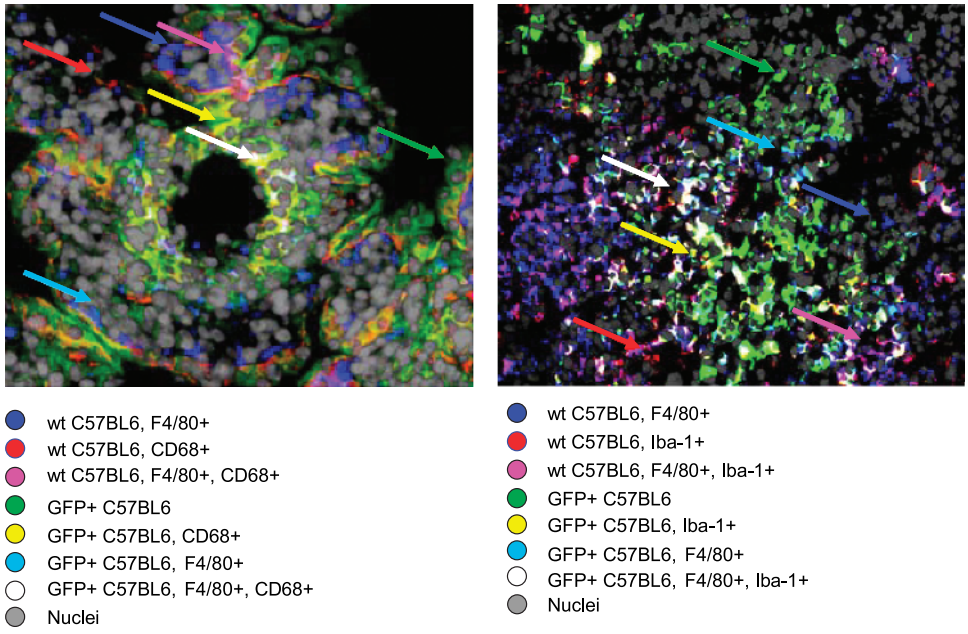

Figure 2. Immunofluorescent analysis of metastases in the brain of normal C57BL/6 mouse parabiosed to transgenic GFP$^+$ mouse. CD68 and Iba-1 were coded red, F4/80 was coded blue, and nuclei were coded gray. Cells from transgenic green fluorescent mice (GFP$^+$) were captured green. Mouse lung tumor metastases in the mouse brain were infiltrated by cells from both the GFP$^+$ mouse and the wild-type C57BL/6 mouse. Infiltrating cells were macrophages from either the wild-type C57BL/6 mouse (blue and pink) or the GFP$^+$ mouse (sky blue and white) and microglial cells from either the wild-type C57BL/6 mouse (red) or the GFP$^+$ mouse (yellow). Infiltrating cells expressing neither CD68/Iba-1 nor F4/80 were also found. Color codes were illustrated in the figure, and cells were indicated by arrows of relevant colors.

and K-1735 melanoma tumor cells, we compared the tumoricidal activity of LPS + IFN-γ–treated macrophages with activated microglia. Both LPS + IFN-γ–treated macrophages and –activated microglia induced similar levels of cytotoxicity (~80%) against the B16-BL6 cells (Figure 3). The K-1735 melanoma cells also exhibited comparable levels of cell death, although that induced by the activated microglia was slightly higher (~75%) than the LPS + IFN-γ–treated macrophages (~50%; Figure 3). Importantly, in two different melanoma cell lines, tumoricidal activity of microglia is potent and equivalent to that of macrophages.

To determine the specificity of microglia-induced cytotoxicity, we examined the effects of these cells on cells from a normal, nontumor origin. Activated microglia did not affect the viability of murine 3T3 fibroblasts and human fibroblasts (Table 1). Notably, activated microglia also had no cytotoxic effects on cells from the brain microenvironment, including immortalized brain endothelial cells and astrocytes (Table 1). To further examine this apparent specificity in microglia-mediated tumor cell cytotoxicity, we cocultured tritiated thymidine-labeled B16-BL6 cells with 3T3 fibroblasts and examined the ability of the microglia cells to induce cytotoxicity in the labeled melanoma cells. As a control, we performed a similar experiment using both tritiated thymidine-labeled 3T3 fibroblasts cultured alone or in combination with B16-BL6 cells. Microglia acted in a tumor cell–specific fashion, selectively killing only the B16 melanoma cells (data not shown). Activated microglia had no cytotoxic effects on 3T3 fibroblasts, cultured either alone or in combination with melanoma tumor cells (data not shown). Taken

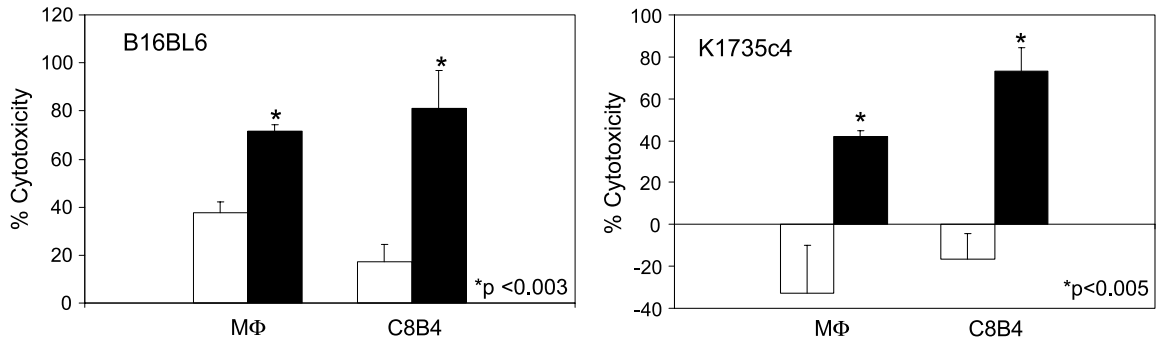

Figure 3. Macrophage/microglia–mediated cytotoxicity against murine melanoma cells. LPS + IFN-γ–activated macrophages and microglia (shaded bars) induced significantly higher levels of cytotoxicity in B16-BL6 and K-1735 C4 cells compared with unactivated microglia/macrophages (unshaded bars). Data are representative of three independent experiments. Percent cytotoxicity ± SD.

Table 1. Murine Microglia Fail to Induce Cytotoxicity in Normal Cells.

Origin	Target Cell	Mean Cytotoxicity (%)
Murine	Brain endothelial cells	−0.1 ± 11.2
	3T3 fibroblasts	−2 ± 9.4
	Astrocytes	−6.3 ± 7.7
Human	Fibroblasts	−1.1 ± 10.7
	Astrocytes	−3.4 ± 9.2

^{3}H-thymidine–labeled target cells in triplicate were cultured alone or with LPS/IFN-γ–activated C8-B4 microglia at a ratio of 1:5. Cells were lysed 72 hours later in 0.1 M KOH, and radioactivity was measured. Percentage cytotoxicity was calculated as the ratio to ^{3}H-thymidine–labeled tumor cells cultured alone. Data are given as mean cytotoxicity ± SD.

together, these observations suggest that the cytotoxic effects produced by microglia are discriminate. That is, activated microglia specifically and selectively induce tumoricidal effects.

Activated microglia can induce cytotoxicity in a variety cell types in various CNS pathologies and in specific cell types during CNS development [25,44–46]. Microglia-derived NO potentially harms cells, and it has been implicated in contributing to oxidative damage and subsequent cell death in a variety of neurologic pathologies [23]. Recent work links microglial-induced neuronal toxicity to iNOS activity and iNOS expression is associated with microglia surrounding brain metastasis in humans [24,25,46]. We examined the activity of iNOS and subsequent production of nitrate, a stable breakdown product of NO in activated and nonactivated microglia and in macrophages. LPS + IFN-γ–activated microglia and macrophages produced significantly more nitrate at all time points measured from 24 to 72 hours (Figure 4). Moreover, previous work from our laboratory has related comparable levels of nitrate to tumor cell cytotoxicity [41]. To test the contribution of NO to the observed microglial-induced cytotoxicity, we pretreated C8-B4 cells with an iNOS inhibitor, NMA, before their activation. Microglia pretreated with NMA failed to induce cytotoxicity in B16-BL6 melanoma cells (Figure 4). These results demonstrate that iNOS activity and subsequent NO production significantly contribute to microglial-induced tumor cell death.

Given the robust cytotoxicity against B16-BL6 mediated by activated microglia, we confirmed their physical interaction by electron microscopy. We observed that multiple microglial cells interact with a single melanoma cell, forming several tether-like contacts with the tumor cell, similar to what is seen between macrophages and tumor cells (data not shown). To determine whether these physical contacts are necessary to produce cytotoxicity, we used a transwell assay system to prevent physical association between activated microglia and melanoma cells but maintain a common medium between the two cell types. Activated microglia produced 85% to 90% cytotoxicity in tumor cells regardless of contact. These data suggest that the factors exchanged between the cells via the medium mediate the cytotoxic effects of microglia. Like macrophages, activated microglia, therefore, induce both direct and indirect cytotoxicity in B16 tumor cells [40].

To prove that the cytotoxic effects mediated by activated microglia were not specific to only melanoma cells, we tested their tumoricidal effects in multiple murine and human cancer cell lines. In all cells tested, we observed microglial induced cytotoxicity, to varying extents (Table 2). No differences were observed between tumor cells from mouse or human origin. The B16-BL6 cells responded most dramatically with 83.4% cytotoxicity, whereas the Lewis lung carcinoma cells, 3LL LM,

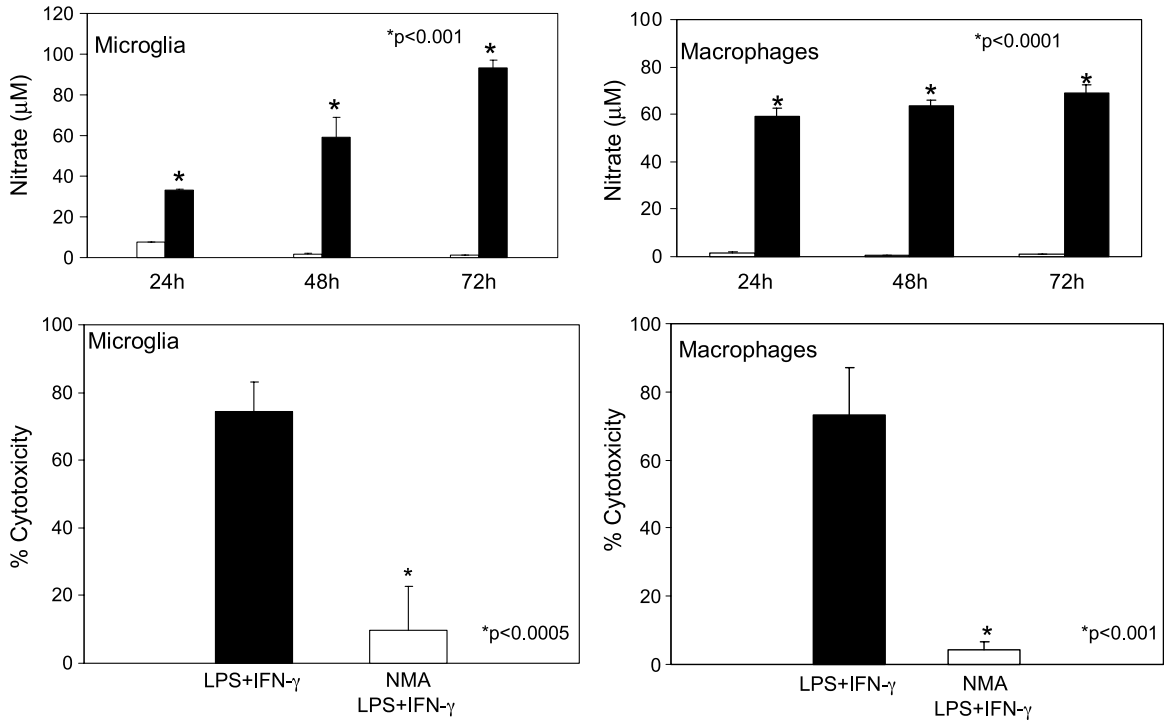

Figure 4. Tumoricidal activity of activated microglia and macrophages is mediated by NO. Unactivated (unshaded bars) and activated (shaded bars) C8-B4 microglia were incubated for 24 to 72 hours before being subjected to the Griess assay. Cell culture supernatants were tested in triplicate for production of nitrate. Data are the representative of 3 independent experiments. Error bars represent SD. *$P < .001$. ^{3}H-TdR–labeled B16 melanoma cells were incubated with either LPS + IFN-γ–activated C8-B4 microglia or LPS + IFN-γ–activated murine macrophages in the presence or absence of 3 mM NMA for 72 hours. NMA reduced the microglial or macrophage mediated cytotoxicity by ~90%. Data are representative of three independent experiments. Error bars represent SD. *$P < .0005$.

Table 2. Murine Microglia–Mediated Cytotoxicity against Tumor Cells.

Origin	Target Cell	Mean Cytotoxicity (%)
Murine	B16-BL6 melanoma	83.4 ± 8.7
	K-1735 C4 melanoma	73.3 ± 11.2
	3LL lung cancer	32.8 ± 3.7
Human	GI101A breast cancer	78.6 ± 4.0
	MDA231P breast cancer	33.7 ± 2.3
	A375P melanoma	68.6 ± 2.7
	U87 glioblastoma	55.0 ± 9.9
	PC14P lung cancer	46.4 ± 11.9

were most resistant to the effects of microglia (32.8% cytotoxicity). Various human breast cancer cells (GI101A, MDA-231P), human lung cancer cells (PC14P), human glioblastoma cells (U87), and mouse (K-1735 C4) and human (A375P) melanoma cells were all susceptible to the tumoricidal effects of activated microglia.

Discussion

Microglia are the major immune effector cells of the CNS and are commonly called the macrophages of the brain [1,2]. Expression of both macrophages and microglia is often associated with experimental and human brain metastases [25–30], we therefore sought to determine whether microglia possess tumoricidal activity *in vitro*. We discovered that indeed LPS + IFN-γ–activated microglia behave much like macrophages and exert tumoricidal effects against various types of cancer cells, confirming previous reports that activated microglia are cytotoxic to metastatic cancer cells [25]. In addition, we observed that activated microglia had no cytotoxic effects on normal cells. The tumoricidal activity of microglia is primarily mediated by the release of NO. We base this conclusion on the data showing that tumor cell cytotoxicity is potently inhibited by the addition of the iNOS inhibitor, NMA. We have previously shown that this mechanism is also responsible for macrophage-induced tumor cell death [41,47]. Whereas functional contacts between microglia and tumor cells were observed using electron microscopy, we discovered that contact between tumor cells and microglia is not a prerequisite to induce cytotoxicity, further implicating the freely diffusible molecule NO in this process. Because microglia possess potent tumoricidal activity *in vitro*, we examined their expression *in vivo* and observed that experimental mouse lung cancer metastases in the brain parenchyma were infiltrated by cells of various subpopulations, including the specialized macrophages, microglia.

Current work in brain metastasis has highlighted the role of cells of the brain microenvironment in this process. The organ microenvironment can alter the ability of tumor cells to "seed" the organ and modify the response of metastatic tumor cells to therapy [48,49]. Recently, our laboratory has characterized the expression and localization of reactive astrocytes surrounding brain metastasis of human cancer cells [26]. Furthermore, we have recently described the chemoprotective role of astrocytes in brain metastasis [50]. In this study, we examined the effects of microglia on tumor cells. Microglia are considered to be the most important immune effector cells in the CNS, but the function of microglia in brain metastasis is not well described. Immunohistochemical analysis of brain metastases in patients reveals expression of activated microglia surrounding areas of tumor burden, and the presence of both macrophages and microglia is widely reported in both experimental and clinical human brain metastases [25–28,30]. We determined the *in vitro* function of microglia by examining the ability of LPS + IFN-γ–activated microglia to induce cytotoxicity in cancer cells. Previous work describes that LPS + IFN-γ–activated microglia exhibit tumoricidal activity against colon cancer cells [51]. Further studies revealed that supernatants from LPS-activated microglia induced apoptosis in metastatic lung cancer cells [25]. Using the C8-B4 microglial cell line, we examined the effects of LPS + IFN-γ–activated microglia on tumor cells and observed microglial-induced cytotoxicity in B16-BL6 and K-1735 C4 melanoma cells that was comparable to that induced by macrophages. Interestingly, activated microglia do not select for "resistant" tumor cells. Tumor cells that survive after being cultured once with activated microglia do not exhibit any acquired resistance to a second round of microglial-induced cytotoxicity (data not shown). In addition, when activated microglia were cultured with cells of normal origin, such as 3T3 fibroblasts, murine astrocytes, and immortalized murine brain endothelial cells, there were no discernable toxic effects (Table 1). Moreover, microglia selectively killed B16-BL6 melanoma cells when the tumor cells were admixed with 3T3 fibroblasts (data not shown). The precise mechanism of the observed specificity of microglia-mediated cytotoxicity is unclear. However, we have previously demonstrated that tumor cells express higher levels of phosphatidylserine (PS) in the outer membrane leaflet, compared with cells of normal origin [15,52]. Interestingly, IFN-γ and LPS-activated monocytes are capable of recognizing elevated levels of PS and targeting these cells for lysis [53]. Because activated microglia largely behave in the same way as activated macrophages, it is likely that PS also serves as a recognition signal for triggering microglial-induced tumor cell death. This mechanism is currently being explored.

On activation, microglia are capable of producing a variety of neuroactive molecules, such as cytokines and chemokines, including IL-1, IL-6, TNF-α, and TGF-β as well as radicals, such as NO and superoxide [52]. A major diffusible mediator that can produce death in adjacent tumor cells is NO, which is regulated by the activity of iNOS [47,54]. Previous work from our laboratory revealed that tumoricidal activity of macrophages is mediated through NO release [41,55]. NO is thought to induce death of neurons near microglia [24]. Furthermore, data suggest that microglia exert cytotoxic effects on colon cancer cells through NO [38]. Indeed, we observed significantly higher levels of nitrate, a stable breakdown product of NO, in both activated microglia and macrophages. We also demonstrate that, like macrophages, the mechanism of microglia-induced tumoricidal activity is mainly due to NO. Inhibition of iNOS activity in either microglia or macrophages nearly completely abrogated the tumoricidal effects on B16-BL6 cells.

On the basis of the specific cytotoxic behavior of microglia on tumor cells *in vitro*, we were interested in observing these cells in a brain metastasis model. Using a parabiosis model, we found the presence of microglia (specialized macrophages) in the lesions formed by metastatic lung cancer. Because this parabiosis model provides common physiologic circulation between wild-type and GFP mice, the origin of cells can be clearly identified by the presence of GFP^+ cells in the brain of wild-type mouse. The finding of $F4/80^+$ cells and GFP^+, $F4/80^+$, $CD68^+$ cells suggested that some circulating monocytes infiltrated these lesions. Importantly, we also found infiltrating cells that expressed neither CD68 nor F4/80. Hence, other inflammatory cells also infiltrate the tumors in the brain. These results confirm that metastases in the brain are infiltrated by both residual cells and circulating cells. Importantly, these data also corroborate previous reports that unlike other glial cells, such as astrocytes and oligodendrocytes that originate in the neuroectoderm, microglia are derived from circulating blood monocytes and are capable of repopulating the brain during pathologic conditions [25,26,30, 44,56–59].

In summary, our results demonstrate that microglia behave nearly identically to macrophages and exhibit selective and specific tumoricidal activity. Our experiments also reveal that microglia, which are derived from circulating mononuclear cells, are recruited to metastases in the brain. To our knowledge, this is the first demonstration of the selective and specific ability of microglia to target tumor cells for cell death. Gaining insight into the interactions between cells of the brain microenvironment, such as microglia, and metastatic tumor cells is extremely important for a better understanding of the biology of brain metastasis.

Acknowledgments

The authors thank Virginia Mohlere for critical editorial comments, Donna Reynolds and Carol Oborn for technical assistance, and Lola López for expert assistance in the preparation of this article.

References

[1] Geissmann F, Manz MG, Jung S, Sieweke MH, Merad M, and Ley K (2010). Development of monocytes, macrophages, and dendritic cells. *Science* **327**, 656–661.

[2] Lawson LJ, Perry VH, Dri P, and Gordon S (1990). Heterogeneity in the distribution and morphology of microglia in the normal adult mouse brain. *Neuroscience* **39**, 151–170.

[3] Nimmerjahn A, Kirchhoff F, and Helmchen F (2005). Resting microglial cells are highly dynamic surveillants of brain parenchyma *in vivo*. *Science* **308**, 1314–1318.

[4] Davalos D, Grutzendler J, Yang G, Kim JV, Zuo Y, Jung S, Littman DR, Dustin ML, and Gan WB (2005). ATP mediates rapid microglial response to local brain injury *in vivo*. *Nat Neurosci* **8**, 752–758.

[5] Perry VH, Hume DA, and Gordon S (1985). Immunohistochemical localization of macrophages and microglia in the adult and developing mouse brain. *Neuroscience* **15**, 313–326.

[6] Alliot F, Marty MC, Cambier D, and Pessac B (1996). A spontaneously immortalized mouse microglial cell line expressing CD4. *Brain Res Dev Brain Res* **95**, 140–143.

[7] Hume DA, Perry VH, and Gordon S (1983). Immunohistochemical localization of a macrophage-specific antigen in developing mouse retina: phagocytosis of dying neurons and differentiation of microglial cells to form a regular array in the plexiform layers. *J Cell Biol* **97**, 253–257.

[8] Perry VH and Gordon S (1987). Modulation of CD4 antigen on macrophages and microglia in rat brain. *J Exp Med* **166**, 1138–1143.

[9] Alliot F, Lecain E, Grima B, and Pessac B (1991). Microglial progenitors with a high proliferative potential in the embryonic and adult mouse brain. *Proc Natl Acad Sci USA* **88**, 1541–1545.

[10] Lawson LJ, Perry VH, and Gordon S (1992). Turnover of resident microglia in the normal adult mouse brain. *Neuroscience* **48**, 405–415.

[11] O'Reilly MS, Holmgren L, Shing Y, Chen C, Rosenthal RA, Moses M, Lane WS, Cao Y, Sage EH, and Folkman J (1994). Angiostatin: a novel angiogenesis inhibitor that mediates the suppression of metastases by a Lewis lung carcinoma. *Cell* **79**, 315–328.

[12] Kaneko YS, Nakashima A, Mori K, Nagatsu T, Nagatsu I, and Ota A (2009). Lipopolysaccharide extends the lifespan of mouse primary–cultured microglia. *Brain Res* **1279**, 9–20.

[13] Qian BZ and Pollard JW (2010). Macrophage diversity enhances tumor progression and metastasis. *Cell* **141**, 39–51.

[14] Pollard JW (2009). Trophic macrophages in development and disease. *Nat Rev Immunol* **9**, 259–270.

[15] Fidler IJ and Schroit AJ (1988). Recognition and destruction of neoplastic cells by activated macrophages: discrimination of altered self. *Biochim Biophys Acta* **948**, 151–173.

[16] Fidler IJ (1985). Macrophages and metastasis—a biological approach to cancer therapy. *Cancer Res* **45**, 4714–4726.

[17] Solis M, Goubau D, Romieu-Mourez R, Genin P, Civas A, and Hiscott J (2006). Distinct functions of IRF-3 and IRF-7 in IFN-α gene regulation and control of antitumor activity in primary macrophages. *Biochem Pharmacol* **72**, 1469–1476.

[18] Romieu-Mourez R, Solis M, Nardin A, Goubau D, Baron-Bodo V, Lin R, Massie B, Salcedo M, and Hiscott J (2006). Distinct roles for IFN regulatory factor (IRF)-3 and IRF-7 in the activation of antitumor properties of human macrophages. *Cancer Res* **66**, 10576–10585.

[19] Yang I, Han SJ, Kaur G, Crane C, and Parsa T (2010). The role of microglia in central nervous system immunity and glioma immunology. *J Clin Neurosci* **17**, 6–10.

[20] Aldinucci D, Gloghini A, Pinto A, De Filippi R, and Carbone A (2010). The classical Hodgkin's lymphoma microenvironment and its role in promoting tumour growth and immune escape. *J Pathol* **221**, 248–263.

[21] Mantovani A, Garlanda C, and Allavena P (2010). Molecular pathways and targets in cancer-related inflammation. *Ann Med* **42**, 161–170.

[22] Yigit R, Massuger LF, Figdor CG, and Torensma R (2010). Ovarian cancer creates a suppressive microenvironment to escape immune elimination. *Gynecol Oncol* **117**, 366–372.

[23] Dringen R (2005). Oxidative and antioxidative potential of brain microglial cells. *Antioxid Redox Signal* **7**, 1223–1233.

[24] Gibbons HM and Dragunow M (2006). Microglia induce neural cell death via a proximity-dependent mechanism involving nitric oxide. *Brain Res* **1084**, 1–15.

[25] He BP, Wang JJ, Zhang X, Wu Y, Wang M, Bay BH, and Chang AY (2006). Differential reactions of microglia to brain metastasis of lung cancer. *Mol Med* **12**, 161–170.

[26] Langley RR, Fan D, Guo L, Zhang C, Lin Q, Brantley EC, McCarty JH, and Fidler IJ (2009). Generation of an immortalized astrocyte cell line from *H-2K^b-ts*A58 mice to study the role of astrocytes in brain metastasis. *Int J Oncol* **35**, 665–672.

[27] Morantz RA, Wood GW, Foster M, Clark M, and Gollahon K (1979). Macrophages in experimental and human brain tumors. Part 2: studies of the macrophage content of human brain tumors. *J Neurosurg* **50**, 305–311.

[28] Morantz RA, Wood GW, Foster M, Clark M, and Gollahon K (1979). Macrophages in experimental and human brain tumors. Part 1: Studies of the macrophage content of experimental rat brain tumors of varying immunogenicity. *J Neurosurg* **50**, 298–304.

[29] Watters JJ, Schartner JM, and Badie B (2005). Microglia function in brain tumors. *J Neurosci Res* **81**, 447–455.

[30] Zhang M and Olsson Y (1995). Reactions of astrocytes and microglial cells around hematogenous metastases of the human brain. Expression of endothelin-like immunoreactivity in reactive astrocytes and activation of microglial cells. *J Neurol Sci* **134**, 26–32.

[31] Yano S, Nokihara H, Hanibuchi M, Parajuli P, Shinohara T, Kawano T, and Sone S (1997). Model of malignant pleural effusion of human lung adenocarcinoma in SCID mice. *Oncol Res* **9**, 573–579.

[32] Hart IR (1979). The selection and characterization of an invasive variant of the B16 melanoma. *Am J Pathol* **97**, 587–600.

[33] Fidler IJ (1980). Therapy of spontaneous metastases by intravenous injection of liposomes containing lymphokines. *Science* **208**, 1469–1471.

[34] Fidler IJ (1973). Selection of successive tumour lines for metastasis. *Nat New Biol* **242**, 148–149.

[35] Kripke ML (1979). Speculations on the role of ultraviolet radiation in the development of malignant melanoma. *J Natl Cancer Inst* **63**, 541–548.

[36] Cailleau R, Young R, Olive M, and Reeves WJ Jr (1974). Breast tumor cell lines from pleural effusions. *J Natl Cancer Inst* **53**, 661–674.

[37] Jat PS, Noble MD, Ataliotis P, Tanaka Y, Yannoutsos N, Larsen L, and Kioussis D (1991). Direct derivation of conditionally immortal cell lines from an *H-2K^b-ts*A58 transgenic mouse. *Proc Natl Acad Sci USA* **88**, 5096–5100.

[38] Kim SJ, Kim JS, Papadopoulos J, Kim SW, Maya M, Zhang F, He J, Fan D, Langley R, and Fidler IJ (2009). Circulating monocytes expressing CD31: implications for acute and chronic angiogenesis. *Am J Pathol* **174**, 1972–1980.

[39] Schackert G and Fidler IJ (1988). Site-specific metastasis of mouse melanomas and a fibrosarcoma in the brain or meninges of syngeneic animals. *Cancer Res* **48**, 3478–3484.

[40] Fan D, Liaw A, Denkins YM, Collins JH, Van AM, Chang JL, Chakrabarty S, Nguyen D, Kruzel E, and Fidler IJ (2002). Type-1 transforming growth factor-beta differentially modulates tumoricidal activity of murine peritoneal macrophages against metastatic variants of the B16 murine melanoma. *J Exp Ther Oncol* **2**, 286–297.

[41] Eue I, Kumar R, Dong Z, Killion JJ, and Fidler IJ (1998). Induction of nitric oxide production and tumoricidal properties in murine macrophages by a new synthetic lipopeptide JBT3002 encapsulated in liposomes. *J Immunother* **21**, 340–351.

[42] Fidler IJ and Nicolson GL (1977). Fate of recirculating B16 melanoma metastatic variant cells in parabiotic syngeneic recipients: brief communication. *J Natl Cancer Inst* **58**, 1867–1872.

[43] Benveniste EN (1998). Cytokine actions in the central nervous system. *Cytokine Growth Factor Rev* **9**, 259–275.

[44] Ransohoff RM and Perry VH (2009). Microglial physiology: unique stimuli, specialized responses. *Annu Rev Immunol* **27**, 119–145.

[45] Wu YP, Mizukami H, Matsuda J, Saito Y, Proia RL, and Suzuki K (2005). Apoptosis accompanied by upregulation of TNF-α death pathway genes in the brain of Niemann-Pick type C disease. *Mol Genet Metab* **84**, 9–17.

[46] Brown GC and Neher JJ (2010). Inflammatory neurodegeneration and mechanisms of microglial killing of neurons. *Mol Neurobiol* **41**(2–3), 242–247.

[47] Xie K, Huang S, Dong Z, Juang SH, Gutman M, Xie QW, Nathan C, and Fidler IJ (1995). Transfection with the inducible nitric oxide synthase gene suppresses tumorigenicity and abrogates metastasis by K-1735 murine melanoma cells. *J Exp Med* **181**, 1333–1343.

[48] Langley RR and Fidler IJ (2007). Tumor cell–organ microenvironment interactions in the pathogenesis of cancer metastasis. *Endocr Rev* **28**, 297–321.

[49] Fidler IJ and Poste G (2008). The "seed and soil" hypothesis revisited. *Lancet Oncol* **9**, 808.

[50] Lin Q, Balasubramanian KK, Fan D, Kim SJ, Guo L, Wang H, Bar-Eli M, Aldape KD, and Fidler IJ (2010). Reactive astrocytes protect melanoma cells from chemotherapy by sequestering intracellular calcium through gap junction communication channels. *Neoplasia* **12**, 748–754.

[51] Murata J, Ricciardi-Castagnoli P, Dessous LE, Martin F, and Juillerat-Jeanneret L (1997). Microglial cells induce cytotoxic effects toward colon carcinoma cells: measurement of tumor cytotoxicity with a γ-glutamyl transpeptidase assay. *Int J Cancer* **70**, 169–174.

[52] Utsugi T, Schroit AJ, Connor J, Bucana CD, and Fidler IJ (1991). Elevated expression of phosphatidylserine in the outer membrane leaflet of human tumor cells and recognition by activated human blood monocytes. *Cancer Res* **51**, 3062–3066.

[53] Rock RB, Gekker G, Hu S, Sheng WS, Cheeran M, Lokensgard JR, and Peterson PK (2004). Role of microglia in central nervous system infections. *Clin Microbiol Rev* **17**, 942–964.

[54] Xie K, Huang S, Dong Z, Gutman M, and Fidler IJ (1995). Direct correlation between expression of endogenous inducible nitric oxide synthase and regression of M5076 reticulum cell sarcoma hepatic metastases in mice treated with liposomes containing lipopeptide CGP 31362. *Cancer Res* **55**, 3123–3131.

[55] Xu L, Xie K, and Fidler IJ (1998). Therapy of human ovarian cancer by transfection with the murine interferon β gene: role of macrophage-inducible nitric oxide synthase. *Hum Gene Ther* **9**, 2699–2708.

[56] Chan WY, Kohsaka S, and Rezaie P (2007). The origin and cell lineage of microglia: new concepts. *Brain Res Rev* **53**, 344–354.

[57] Napoli I and Neumann H (2009). Microglial clearance function in health and disease. *Neuroscience* **158**, 1030–1038.

[58] Davoust N, Vuaillat C, Androdias G, and Nataf S (2008). From bone marrow to microglia: barriers and avenues. *Trends Immunol* **29**, 227–234.

[59] Davoust N, Vuaillat C, Cavillon G, Domenget C, Hatterer E, Bernard A, Dumontel C, Jurdic P, Malcus C, Confavreux C, et al. (2006). Bone marrow $CD34^+/B220^+$ progenitors target the inflamed brain and display *in vitro* differentiation potential toward microglia. *FASEB J* **20**, 2081–2092.